2020-01-2053

Knock Mitigation Effectiveness of EGR Across the Pressure-Temperature Domain

Author, co-author (Do NOT enter this information. It will be pulled from participant tab in MyTechZone)

Affiliation (Do NOT enter this information. It will be pulled from participant tab in MyTechZone)

Abstract

Exhaust gas recirculation (EGR) has been shown to enable efficiency improvements in SI engines through multiple different mechanisms, including decreasing the knock propensity at high load, which allows higher compression ratio. While many of the benefits of EGR are applicable to both low and high power density engines, including reductions in pumping work and improved specific heat ratio, the knock benefits and corresponding compression ratio increases have been limited to low power density naturally aspirated engines primarily intended for hybrid vehicle architectures. An earlier study [1] indicated that there may be a kinetic limitation for the ability of EGR to mitigate knock under these conditions, but that study only considered a small number of conditions. This investigation expands on that study while also providing data for model validation for the new light-duty combustion consortium from the U.S. Department of Energy: Partnership for Advancing Combustion Engines (PACE). In this investigation, the effectiveness of EGR to mitigate knock is studied with regards to the effect of engine speed (1,500 and 3,000 rpm), changing trajectory in the pressure-temperature domain by varying the intake manifold temperature (35, 60, and 90 deg C), and by considering the effect of minor species by studying the effect of untreated EGR vs. EGR that has been treated by an automotive three-way catalyst. Additionally, to increase the relevance of these data for future modeling studies, the performance of the full boiling range gasoline was compared relative to a surrogate formulation. The study found that the fuel surrogate performs well, confirmed the kinetic limitations of EGR to mitigate knock under boost, and showed improvements in EGR performance with catalyzed EGR.

Introduction

Many of the benefits of cooled exhaust gas recirculation (EGR) on engine efficiency for spark-ignited engines were previously reviewed by Szybist et al. [1] and are included here for completeness.

Cooled EGR is an attractive option to increase engine efficiency in spark-ignited engines because it offers well-understood thermodynamic advantages while maintaining compatibility with conventional three-way catalyst (TWC) aftertreatment. The thermodynamic efficiency advantages for high EGR strategies are described in detail in a modeling study by Caton [2], and are summarized below. First, additional mass from the EGR causes the manifold pressure to increase without increasing the intake oxygen flow, which at part-load conditions can decrease engine pumping and increase engine efficiency. Second, the peak in-cylinder temperature decreases with EGR, causing the in-cylinder heat transfer to decrease. Third, due to combined thermal and composition effect, the working fluid ratio of specific heats (γ) increases with EGR, increasing efficiency. In addition to these thermodynamic advantages, EGR also reduces the exhaust temperature which can reduce the need for overfueling at high engine speeds [3-5].

The last beneficial effect of EGR that will be discussed, and the main focus of this study, is that EGR can reduce knock propensity in SI engines [3, 4, 6-8]. This can enable increased engine efficiency, either through advancing the combustion phasing at high loads, or by increasing the compression ratio of the engine for a full-map efficiency benefit. In this respect, Alger et al. [6] concluded that every ~1 % EGR was equivalent to a 0.5 octane number increase, and that at an engine load of 8 bar brake mean effective pressure (BMEP), it was possible to advance the combustion phasing by 15 crank angle degrees (CAD) with the use of 20% EGR.

This reduction in knock propensity with EGR has been one of the enabling technologies for the highest efficiency stoichiometric SI engines ever produced for the light-duty sector, achieving a peak brake thermal efficiency of 40% from Hyundai-Kia Corporation [9] and from Toyota [10, 11]. Additionally, the Toyota engine described by Hakaryia et al. [10] was later benchmarked by the U.S. EPA [12] who provide a more complete description of the operating conditions. Further efficiency improvements have been achieved in prototype engines by Lee et al. [13] who achieved 42.2% brake thermal efficiency, and Ikeya et al. project 45% brake thermal efficiency based on single cylinder engine results. In all of these studies, the knock-suppression effects of EGR were cited.

The engines that have taken advantage of the knock-suppression benefits of EGR to increase the compression ratio are naturally aspirated and have low power density (LPD), two of which are specifically designed to be used in hybrid powertrains [9, 11]. This LPD pathway to higher vehicle efficiency is one of the major routes to achieving higher vehicle efficiency, with the other being a high power density (HPD) route that relies on engine downsizing and downspeeding. These routes are compared for engines of similar power output by Szybist et al. [14] who showed that both routes are viable paths to achieve efficiency benefits relative to a baseline engine technology, with HPD engines having an efficiency advantage at low torque, and LPD engines having an efficiency advantage at higher torque.

Extending the knock-suppression benefits of high EGR combustion strategies to HPD engines, if possible, is desirable. HPD engines typically have a significantly lower compression ratio [14], and HPD engines are a growing share of engines in the marketplace, with the sale of boosted engines increasing from 1.7% in 2005 to 30.8% in 2018 in the U.S. In contrast, during that same time period, hybrid electric vehicles that are best-suited for the LPD engines increased from about 1% to a maximum of 4% of market share in the U.S. [15]. Additionally, both GM and VW announced August of 2019 that they would no longer make hybrid electric vehicles [16]. Thus, if the knock suppression benefits of EGR can be extended to include HPD engines, this technology could have a much larger impact than it currently has with just LPD engines.

However, there is early evidence that shows that the same magnitude of knock suppression for LPD engines is not possible for HPD engines. At an engine load of 14 bar indicated mean effective pressure (IMEP), Hoepke et al. [17] found that while EGR still provided a substantial knock-mitigation effect, about 8 CAD advance in spark timing and combustion phasing with 20% EGR, it was only about half of what was reported by Alger et al. [6]. Lewis et al. [18] investigated EGR knock mitigation effects at a constant intake manifold density and found they were able to advance spark by as much as 10 CAD at loads over 20 bar BMEP, but this dataset was also accompanied by a decrease in load with EGR, which is a direct result of maintaining a constant intake density. Splitter and Szybist [19] investigated the effect of EGR across the operating load range with three different fuels. While they found a significant attenuation in knock propensity at engine loads below 12 bar IMEP with the use of EGR, the ability to advance combustion phasing when EGR was added at high loads diminished to the point where nearly no benefit was observed at loads above 15 bar IMEP.

This trend of a decreasing effectiveness of EGR to mitigate knock under boosted operating conditions was elucidated by Szybist et al. [1]. They showed that the effectiveness of EGR on knock mitigation was related to pressure-temperature trajectory of the fuel and air mixture. Under naturally aspirated conditions, which produces a pressure-temperature trajectory similar to the research octane number (RON) test [20], the autoignition delay increases as EGR is added, as calculated at constant volume using a detailed chemical kinetic mechanism. However, under boosted operating conditions when the pressure-temperature trajectory can be categorized as “beyond RON,” meaning that the cylinder temperature is lower than the RON test for a given pressure, EGR does not have a substantial kinetic effect. The concept of engine conditions being “beyond RON” or “beyond MON” was pioneered by Kalghatgi in the development of the octane index [21]. Thus, they concluded that there was a kinetic limitation in the use of EGR to suppress knock for boosted operating conditions.

While the earlier study by Szybist et al. [1] made a strong case that this kinetic limitation existed, it was based on a relatively small amount of experimental data at one engine speed, and only with EGR that had not been treated with an exhaust three-way catalyst. The purpose of this study is to expand upon this earlier investigation and study the effectiveness of EGR to mitigate knock at multiple engine speeds (1,500 and 3,000 rpm), changing trajectory in the pressure-temperature domain by varying the intake manifold temperature (35, 60, and 90 deg C), and by considering the effect of minor species by studying the effect of treating EGR with a TWC. Further, to ensure that this data is applicable to future kinetic and CFD modeling studies within the PACE initiative, the engine performance is compared with a 7-component surrogate fuel.

Methodology

Experimental Facility

The experimental apparatus and much of the methodology used in this study has been previously reported [1, 22, 23]. A 2.0 L GM Ecotec LNF engine equipped with the production side-mounted direct injection fueling system was used. Engine geometry details are presented in Table 1. The engine was converted to a single-cylinder engine by disabling cylinders 1, 2, and 3. The combustion chamber geometry and camshaft profiles were unchanged from the stock configuration. As EGR was added, no attempt was made to re-optimize camshaft phasing. The engine was operated using the stock GDI fuel pump and a constant fuel rail pressure of 125 bar was maintained throughout this study.

Table 1 Engine geometry.

Bore × Stroke [mm]	86.0 × 86.0
Conrod length [mm]	145.5
Wrist pin offset toward expansion stroke[mm]	0.8
Compression ratio [-]	9.2 : 1
Fuel injection system	Direct injection, side-mounted, production injector with opposite linear wall directed six-hole spray pattern

A laboratory air handling system capable of EGR and boosted operation was used. Pressurized and dried facility air having less than 5% relative humidity was metered to the engine using an Alicat mass flow meter (MCP-1500SLPM-D-54X54/5M). Electromechanical backpressure and EGR valves from Flowserve were used to control the backpressure and EGR. At all conditions, the backpressure was maintained at 10 kPa higher than the intake pressure to enable EGR

flow from the exhaust surge tank to the intake surge tank. An optional TWC can be installed in the exhaust system under some conditions or replaced with exhaust tubing to investigate the differences between catalyzed or uncatalyzed EGR. The TWC has a volume of 1.3 L and is from a PZEV 2009 Chevy Malibu. This catalyst was used in previous dyno studies for more than 100 hours and was previously used in a study by Prikhodko et al. [24].

The coolant loop used an external water pump, heater, and heat exchanger arrangement. This allowed the engine block to be pre-heated prior to starting the engine. During engine operation, the engine-out coolant temperature was controlled to 90°C at all operating conditions. The internal oil pump was used for oil delivery, but an external heat exchanger was used to control the engine-out oil temperature to 90°C. The EGR loop used in this study was held above its dew point to prevent water condensation (≥70°C upstream mixing with the intake air). EGR was measured using a model EGR5230 from ECM, a non-intrusive method that utilizes pressure-compensated wideband oxygen sensors in both the intake and exhaust.

A custom engine controller was used, utilizing hardware from National Instruments Powertrain Controls platform. Combustion analysis was done using software developed in-house, Oak Ridge Combustion Analysis System (ORCAS). Crank-angle resolved data were collected using an AVL 365C shaft encoder. For each experimental condition, cylinder pressure, spark discharge, injector command, intake and exhaust manifold pressure, and intake and exhaust camshaft position data were recorded for 1,000 consecutive cycles at 0.2°CA resolution for the 1,500 rpm operating conditions and 0.4°CA resolution for the 3,000 rpm operating conditions due to data throughput constraints. Cylinder pressure was measured using a flush-mounted Kistler 6125C piezoelectric pressure transducer, and camshaft position was recorded from the production hall-effect sensors. Crank-angle resolved intake and exhaust manifold pressures were measured using Kistler 4011A and 4049B transducers, respectively. For each cycle, trapped mass was calculated using the cam position sensor feedback with in-cylinder pressure and by applying the method described by Yun and Mirsky [25] with the measured polytropic expansion coefficient. Apparent heat release was then solved using the zero-phase-filtered in-cylinder pressure and the individual cycle trapped mass with the approach described by Chun and Heywood and temperature was solved using the ideal gas law [26].

Start of fuel injection timing was commanded during the intake stroke and was held constant at -280 CAD after firing top dead center ($aTDC_f$). Spark timing was adjusted as needed to achieve the desired combustion phasing, and spark dwell was held constant with the stock ignition coil at 2.8 ms to maintain constant ignition energy. To prevent hot-spot runaway at high load, a spark plug two heat ranges colder than the production engine's plug was used. The colder spark plug is not directly available from the engine or factory original spark plug manufacturer; rather it was identified through cross-referencing current production spark plugs with the same thread and reach as the factory original spark plug. A Denso Iridium HP spark plug was identified as being compatible and was used throughout the study. Engine fuel flow was measured with a Micromotion CMF010 coriolis-based fuel flow meter.

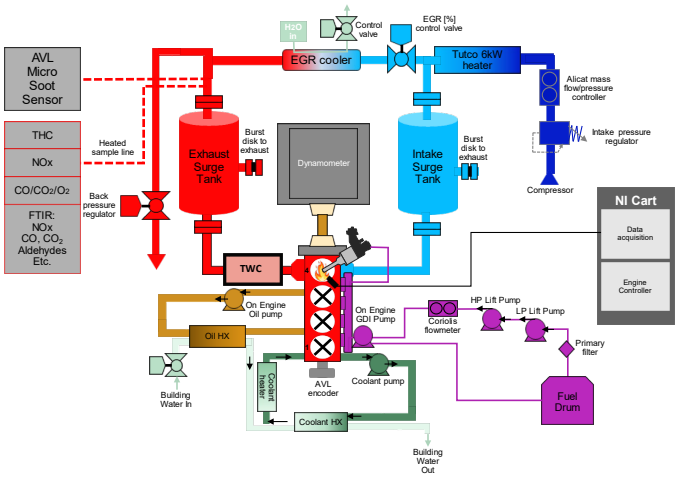

Figure 1. Schematic of the engine air handling system.

Fuels Investigated

This work was done as part of DOE-funded Partnership to Advance Combustion Engines (PACE) Consortium. Two objectives of this initiative are 1) to reduce the knock propensity of stoichiometric SI engines, and 2) to improve combustion modeling, including predictive simulation of the knock-limited combustion phasing. While the majority of this study focuses on the former, this investigation also supported the latter by comparing the performance of a research gasoline to a surrogate fuel formulation.

The gasoline used is from Gage Products, has a product name of RD5-87, and is a reproducible research-grade gasoline intended to be representative of regular-grade E10 gasoline in the U.S. The surrogate for this fuel was designed by colleagues at Lawrence Livermore National Laboratory who are also working on the PACE Consortium. They used a multi-objective approach to match autoignition metrics, carbon, hydrogen, chemical class, and boiling point, as detailed in Wagnon et al. [27]. The composition of the surrogate, named PACE-1, contains 7 components. This surrogate fuel was hand-blended for this study, and the desired concentrations (as defined by Wagnon et al. [27]) and the actual as-blended concentrations of each component are shown in Table 2.

Table 2. Formulation of the PACE-1 gasoline surrogate desired composition, as specified by Wagnon et al. [27], and the actual composition as-blended and used in this study.

	Desired Mass %	Actual Mass %	Error %
n-heptane	17.13	17.12	-0.06
iso-pentane	6.35	6.37	0.37
iso-octane	19.89	19.90	0.05
1-hexene	5.97	5.97	-0.06
Cyclopentane	10.60	10.60	-0.03
1,2,4-trimethylbenzene	30.11	30.09	-0.06
Ethanol	9.95	9.95	0.03

The purpose of blending the surrogate composition was to confirm that it produced similar performance as the baseline fuel, both in terms of the measured fuel properties and in terms of the fuel performance in the engine. This confirmation is a necessary step so that the physical properties and kinetic mechanisms for the surrogate can be used for kinetic and for computational fluid dynamics (CFD) modeling studies. The fuel properties of the RD5-87 gasoline and the PACE-1 surrogate are shown in Table 5. As can be seen, all the measured fuel properties of the surrogate and reasonably close to those of the gasoline fuel.

Table 3. Fuel properties of RD5-87 and the physical surrogate.

	Method	Gasoline RD5-87	Surrogate PACE-1
Research Octane Number [-]	ASTM D2699	92.3	92.3
Motor Octane Number [-]	ASTM D2700	84.6	82.4
Octane Sensitivity [-]	RON – MON	7.7	9.9
Initial boiling point [°C]	ASTM D86	40.4	44.4
T10 [°C]	ASTM D86	54.8	59.4
T50 [°C]	ASTM D86	101.3	98.9
T90 [°C]	ASTM D86	157.9	165.0
Final boiling point [°C]	ASTM D86	172.1	165.6
Specific Gravity [-]	ASTM D4052	0.75	0.75
Carbon [wt %]	ASTM D5291	82.67	82.52
Hydrogen [wt %]	ASTM D5291	13.66	13.65
Oxygen [wt %]	ASTM D5599	3.51	3.38
Stoichiometric Air-Fuel Ratio	Calculated	14.2	14.5
Lower Heating Value [MJ/kg]	ASTM D4809	41.93	41.81
Aromatics [wt %]	ASTM D6729	27.9	30.3
n-Saturates [wt %]	ASTM D6729	13.9	17.2
Iso-Saturates [wt %]	ASTM D6729	29.0	26.2
Olefins [wt %]	ASTM D6729	5.5	5.8
Naphthenes [wt %]	ASTM D6729	12.4	10.2
Ethanol [wt %]	ASTM D5599	10.12	9.74

Engine Operating Conditions

The engine operating conditions investigated are shown in Table 4. Operating conditions were set by selecting the desired intake temperature and knock-limited CA50 combustion phasing. At each condition, intake manifold pressure was adjusted with a stoichiometric air/fuel ratio to achieve the desired knock-limited combustion phasing, thus intake manifold pressure and engine load were not independent variables in designing this matrix, but rather determined by the knock propensity. Spark timing was adjusted as needed. The resultant intake manifold pressure without EGR is shown in Table 4. As EGR was introduced, the air and fuel flow rate for that condition were held constant, thus intake manifold pressure increased with EGR. The knock-limited CA50 combustion phasing is defined as the combustion phasing at which the 10% of engine cycles with the highest maximum amplitude of pressure oscillation (MAPO) have an average MAPO equal to the threshold value. The allowable MAPO value increases with engine speed such that a MAPO value of 30 kPa was used at 1,500 rpm and a MAPO value of 60 kPa was used at 3,000 rpm.

Table 4. Engine operating conditions investigated in this study.

Condition	Engine Speed [rpm]	CA50 Combustion Phasing [CA aTDC$_f$]	Intake Temperature [°C]	Intake Pressure w/o EGR[kPaa]
Condition 1	1,500	25	35	145
Condition 2	1,500	15	35	99
Condition 3	1,500	25	60	131
Condition 4	1,500	25	90	113
Condition 5	3,000	25	35	166
Condition 6	3,000	15	35	113
Condition 7	3,000	25	60	150
Condition 8	3,000	25	90	131

EGR sweeps were only conducted for each operating condition for the RD5-87, and not for the surrogate. The surrogate fuel was tested at only 0% EGR conditions. The EGR sweeps were carried out in the following manner:

- During the EGR sweep, air and fuel rate were held constant
- EGR was added up to 20% EGR or a coefficient of variation (COV) of IMEP limit of 4%
- Spark timing was adjusted to achieve the desired threshold MAPO
- Engine load was allowed to vary through the EGR sweeps.

Results

Baseline Operating Conditions

In the Methodology section, the engine operating conditions were described in terms of the desired knock-limited combustion phasing for each operating condition and the engine load was allowed to float. These data are shown graphically in Figure 2 and Figure 3 as net IMEP vs. the CA50 combustion phasing. At each engine speed, there is effectively 3-point temperature sweep at constant combustion phasing, and a 2-point combustion phasing sweep at constant intake temperature. Net IMEP floats and is between 10 and 21 bar at all operating points.

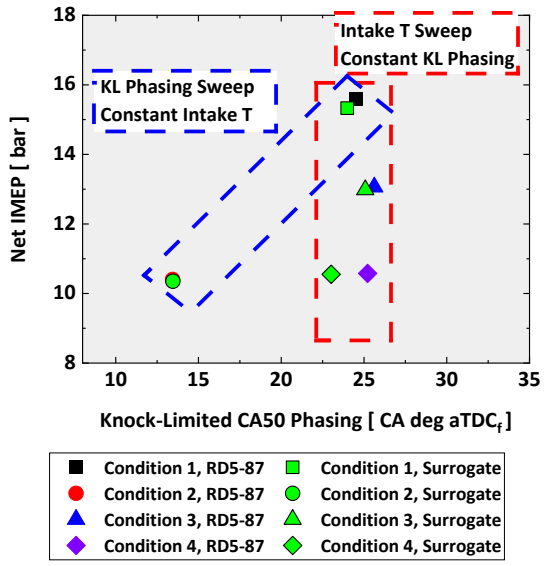

Figure 2. Net IMEP as a function of the knock-limited CA50 combustion phasing at 1,500 rpm (Conditions 1-4) for the RD5-87 gasoline and the surrogate fuel.

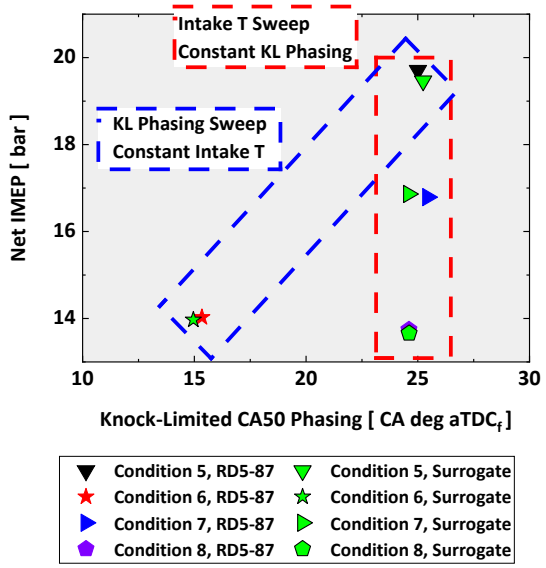

Figure 3. Net IMEP as a function of the knock-limited CA50 combustion phasing at 3,000 rpm (Conditions 5-8) for the RD5-87 gasoline and the surrogate fuel.

These operating conditions successfully provided a range of pressure-temperature trajectories, which as discussed in the Introduction section, was one of the main motivations of this investigation. This is shown in Figure 4, where the pressure-temperature trajectories range from the Beyond RON to the RON-like conditions. From the standpoint of knock-limited operation, this is the desired pressure-temperature range to be investigating knock-limited operation. The work from Szybist et al. [1] illustrated that, while typical SI engines do have pressure-temperature trajectories between RON and MON, and even, beyond MON, those operating conditions typically are not knock-limited, and thus do not represent operational barriers. It is also interesting to note that there are nearly identical pressure-temperature trajectories for Condition 2 and Condition 4 (refer to Table 4) despite very different engine operating conditions. This similarity in pressure-temperature trajectory will be revisited when evaluating the effectiveness of EGR to mitigate knock.

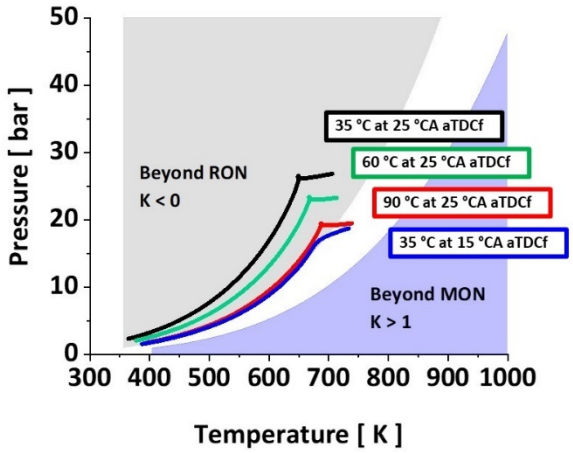

Figure 4. Illustration of the pressure-temperature conditions investigated. Data shown at 1,500 rpm without EGR.

Figure 2 and Figure 3 also show the performance of the fuel surrogate. As discussed in the Methodology section, it is important that the surrogate reproduce the performance of the real fuel over a wide range of operating conditions to confirm its suitability for modeling purposes. The surrogate fuel is shown with the green markers and performs in a nearly identical manner to the fully formulated fuel, despite the differences in the RON and MON numbers noted in Table 3. The exception to this is a 2 CAD more advanced combustion phasing for the surrogate fuel at 1,500 rpm and 90°C intake temperature.

In addition to ensuring that the knock-limited CA50 combustion phasing is similar, it was also desirable to ensure similar cyclic variability for the surrogate and the full boiling range RD5-87 gasoline. This is shown graphically for cylinder pressure at two different operating conditions: Figure 5 shows Condition 1 and Figure 6 shows Condition 8. Both conditions show good agreement between the baseline fuel and surrogate, not only for the average performance represented by the solid line, but also for the variability, where the shaded area represents two standard deviations from the mean.

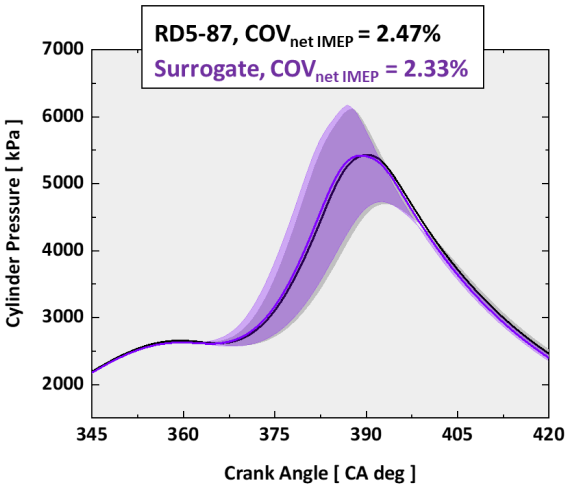

Figure 5. Cylinder pressure of two repeats of RD5-87 and the surrogate fuel for Condition 1 with 0% EGR. Shading represents two standard deviations of the mean.

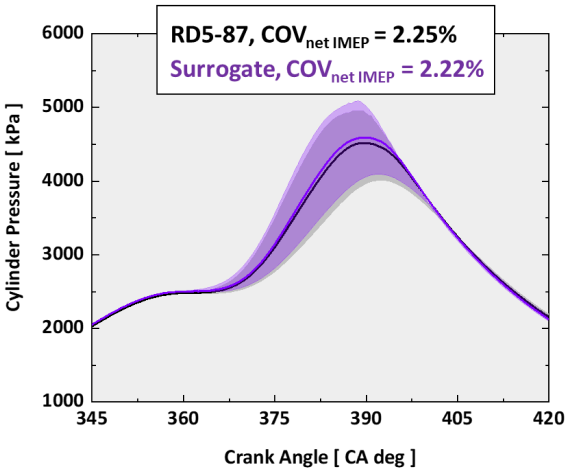

Figure 6. Cylinder pressure for RD5-87 and the surrogate fuel for Condition 8 with 0% EGR. Shading represents two standard deviations of the mean.

Based on the agreement between the fully formulated RD5-87 gasoline and the surrogate, it can be concluded that both the knock-limited combustion phasing, engine load, and cyclic variability are reproduced well. Thus, the use of this surrogate formulation for RD5-87 gasoline is recommended moving forward.

Effect of Three-Way Catalyst on Engine Performance and Emissions

Prior to assessing knock propensity differences for EGR that has or has not been treated with a TWC, we must first develop an understanding of the effects that the physical presence of the TWC has on the knock-limited engine operation. Figure 7 shows the engine exhaust under two different conditions: a) without the TWC, and b) with the TWC.

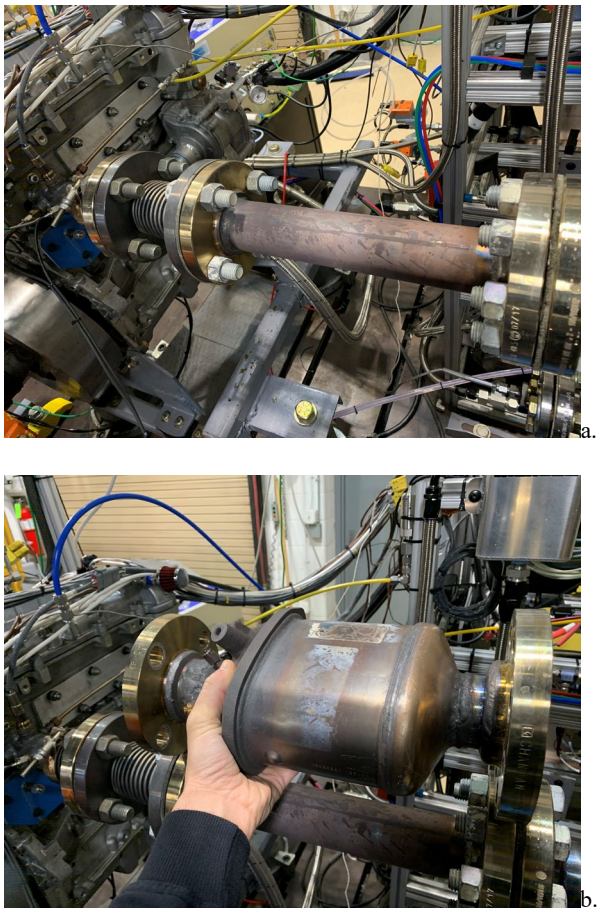
a.

b.

Figure 7. Photographs of the engine exhaust with a) the exhaust pipe without a TWC, and b) photograph showing the TWC that can be installed in the exhaust.

The presence of the TWC in the exhaust changed the knock-limited combustion phasing, as shown in Figure 8 for 1,500 rpm operation (Conditions 1-4) and Figure 9 for 3,000 rpm operation (Conditions 5-8). At 1,500 rpm (Figure 8), the knock-limited combustion phasing was retarded by a significant amount for all of the operating conditions, including by more than 5 CAD at the two highest intake temperature operating conditions. In contrast, at 3,000 rpm (Figure 9) the knock-limited combustion phasing was retarded by less than 3 CAD despite the flow through the catalyst being nominally doubled relative to the 1,500 rpm conditions. Thus, the difference does not increase with higher flow, and therefore higher backpressure, over the TWC. The cause of this discrepancy either has to do with exhaust tuning (i.e., constructive and destructive pressure wave interference causing higher trapped residuals), or is kinetic in nature (i.e., the operating conditions at 3,000 rpm may not be as sensitive to higher backpressure and higher trapped residuals). Regardless of the cause,

the effectiveness of EGR to mitigate knock must be measured from the 0% EGR case for that configuration (with or without the TWC).

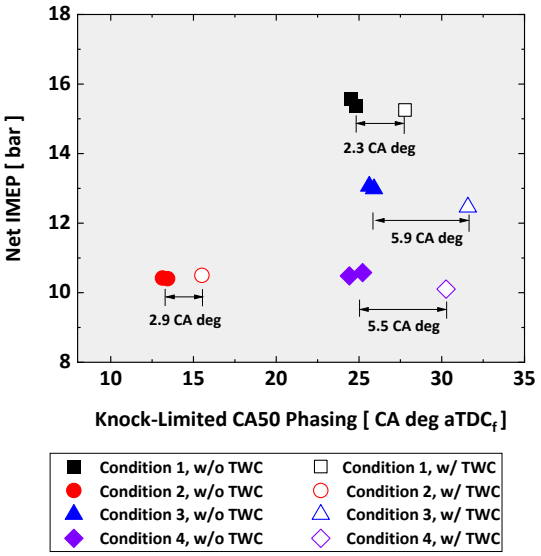

Figure 8. Net IMEP as a function of the knock-limited CA50 combustion phasing at 1,500 rpm (Conditions 1-4) to illustrate the effect of the TWC with 0% EGR.

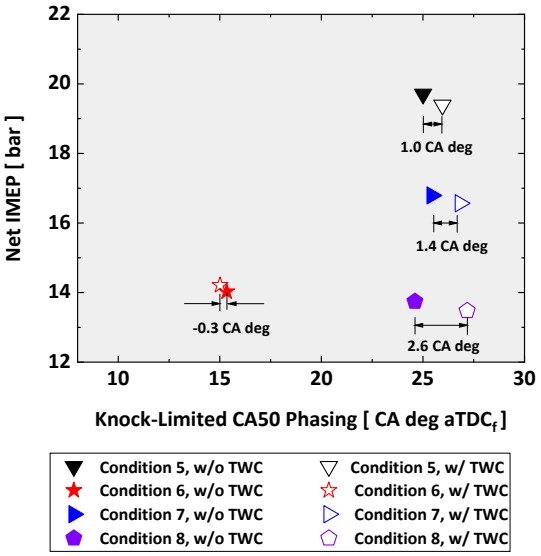

Figure 9. Net IMEP as a function of the knock-limited CA50 combustion phasing at 3,000 rpm (Conditions 5-8) to illustrate the effect of the TWC with 0% EGR.

Figure 10 shows a representative example of the change in exhaust emissions with the TWC. In this example, the NOx and HC emissions were reduced by approximately 97% and the CO emissions were reduced by 92%. This level of TWC effectiveness is significantly lower than what would be expected in a production engine because the engine control strategy did not include dithering, a practice used in production engines that adjusts the air/fuel ratio slightly lean and then slightly rich to maximize TWC effectiveness. Nonetheless, these levels of reductions of exhaust emissions are large and represent a significant contrast to investigate changes in EGR reactivity on knock.

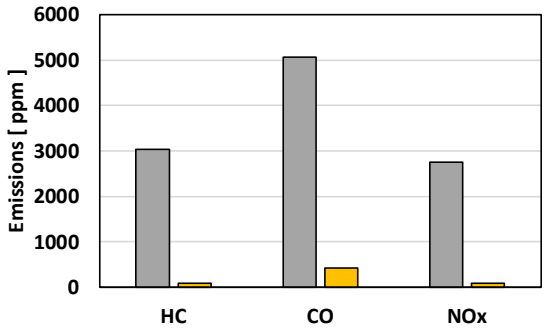

Figure 10. Gaseous emissions before and after the TWC at Condition 1 (1,500 rpm, 35°C intake temperature, CA50 = 25 CAD aTDCf).

Theoretical Effects of EGR on Knock

In order to interpret the experimental results, it is useful to set expectations by first reviewing the competing theoretical effects of EGR addition on knock propensity. The first effect is that, relative to a stoichiometric air and fuel mixture, the addition of EGR raises the ratio of specific heats, or γ. This is shown as a function of temperature for a stoichiometric mixture of iso-octane with and without 20% EGR in Figure 11. The higher γ for an EGR mixture results in a higher temperature and pressure during the compression process. Thus, when EGR is added, the unburned air and fuel mixture is exposed to higher temperatures, even when the temperature at the start of compression is maintained constant.

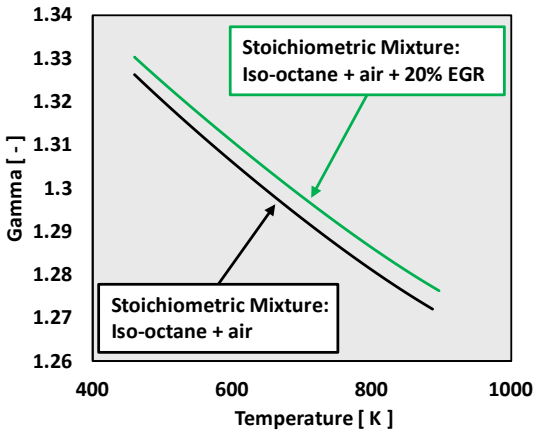

Figure 11. Gamma of stoichiometric mixtures of iso-octane and air with and without 20% EGR as a function of temperature.

The second factor that needs to be considered is that the addition of EGR increases the pressure in the cylinder. This is because the EGR does not displace the air and fuel mixture but is instead added to the cylinder contents. In practice, since EGR increases engine efficiency, the mass of air and fuel will decrease to some extent. However, for illustrative purposes, we will assume that the fueling rate is maintained constant.

The increased pressure at the start of compression for EGR operation changes the pressure-temperature trajectory relative to the baseline condition. The combined effect of a higher γ and a higher pressure at the start of compression is shown in Figure 12, and is a figure that

was originally published by Szybist et al. [1]. This plot shows that relative to the 0% EGR conditions (solid lines), the addition of 20% EGR causes the compressed gas temperature and pressure at TDC to increase by up to 35 K and 7 bar. Thus, these first two factors of higher cylinder mass and higher γ both serve to increase the knock propensity.

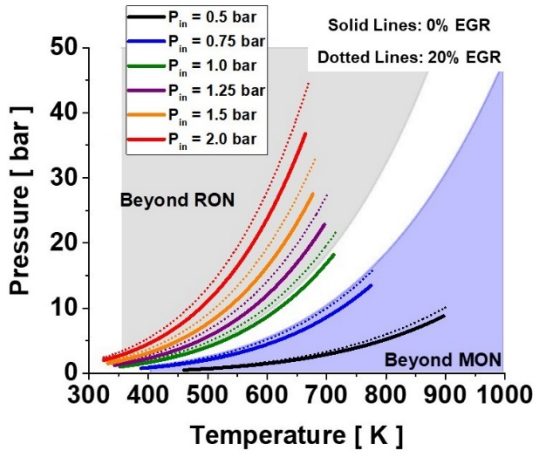

Figure 12. Pressure-temperature trajectories during the compression stroke with and without 20% EGR for a series of intake manifold pressures. Originally published by Szybist et al. [1]

Next, the presence of EGR reduces flame speed and increases the duration of the combustion process [28-30]. This changes the pressure-temperature trajectory of the end gas in the combustion chamber such that the compressive heating from the deflagration starts earlier in the combustion chamber as a result of spark timing being advanced to maintain constant CA50 combustion phasing, causing the fuel and air mixture to experience increased temperatures earlier in the cycle. However, the slower combustion event leads to a comparable peak pressure to the 0% EGR case, despite the higher cylinder mass [28]. Thus, the net directional effect of the slower combustion duration on knock propensity is not clear.

Finally, the presence of EGR, and particularly the lower concentration of O_2 and fuel in the mixture, can reduce the kinetic reactivity of the mixture. As was discussed in Szybist et al. [1], this kinetic effect is not equal at all operating conditions. Instead, they reported that the kinetic effect of mitigation was much more effective under naturally aspirated condition. At pressure-temperature conditions in the Beyond RON region, which correspond to boosted engine operation, there kinetic effect was attenuated. This is shown in Figure 13 using a higher-RON fuel than is used in the current investigation, which was originally published by Szybist et al. [1]. The kinetic modeling performed in that study represented constant volume ignition delays for multi-component surrogates for three different high-octane gasolines (RON = 98), and included 150 ppm NO in the gas mixture regardless of EGR level.

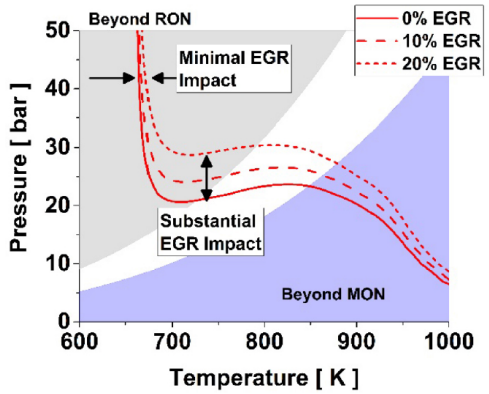

Figure 13. Constant volume ignition delay contours of 8 ms across the pressure-temperature space using 0, 10, and 20% EGR using a high RON gasoline (RON = 98), originally published by Szybist et al. [1].

Experimental Effects of EGR on Knock

Unlike the previous work by Szybist et al. [1], this study was designed to experimentally investigate a wider range of the pressure-temperature domain, and to include the effect of the minor constituents in EGR on knock propensity. The knock-limited CA50 combustion phasing sweeps are shows in Figure 14 and Figure 15 both with and without the use of the TWC. As shown in Figure 8, the physical presence of the TWC in the exhaust changed the knock propensity of the engine. Thus, there is a difference in the knock-limited combustion phasing for 0% EGR. For both the untreated and TWC-treated EGR, the addition of EGR does allow combustion phasing to be advanced. Note that when EGR was added, air and fuel flow rate were held constant, resulting in an increase in load with EGR. The extent to which the combustion phasing can be advanced is dependent both on the operating condition and whether or not the EGR was treated with the TWC.

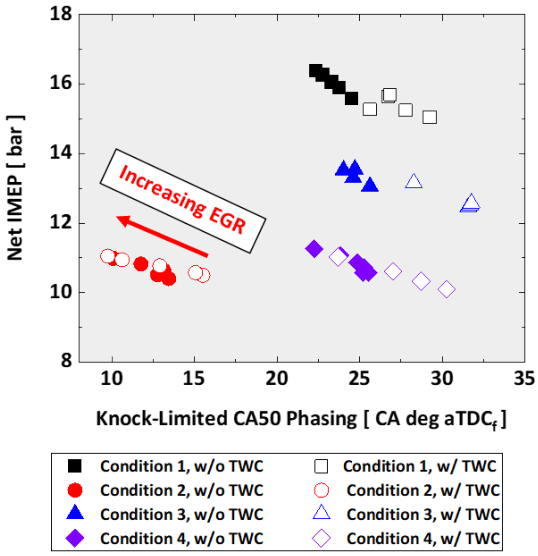

Figure 14. Net IMEP as a function of the knock-limited CA50 combustion phasing at 1,500 rpm (Conditions 1-4) over an EGR sweep for using untreated or TWC-treated EGR.

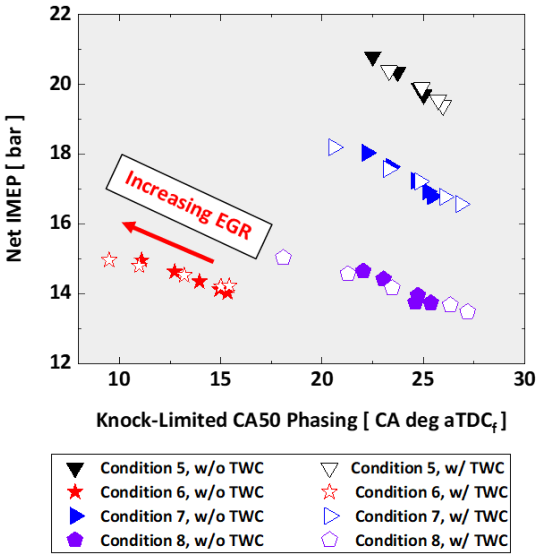

Figure 15. Net IMEP as a function of the knock-limited CA50 combustion phasing at 3,000 rpm (Conditions 5-8) over an EGR sweep for using untreated or TWC-treated EGR.

The advance of CA50 combustion phasing as a function of EGR is shown in Figure 16 for the 1,500 rpm conditions and in Figure 17 for the 3,000 rpm conditions. The CA50 combustion phasing is observed to be approximately linear for all conditions, but the slope is dependent on the condition and whether or not the EGR was treated with the TWC. These slopes are quantified for each operating condition by linear regression and presented in Table 5. In all cases, the effectiveness of EGR for mitigating knock increases with the TWC-treated EGR, and in some cases the TWC-treated EGR is more than twice as effective as the untreated EGR in mitigating knock. Additionally, there are significant differences between operating conditions.

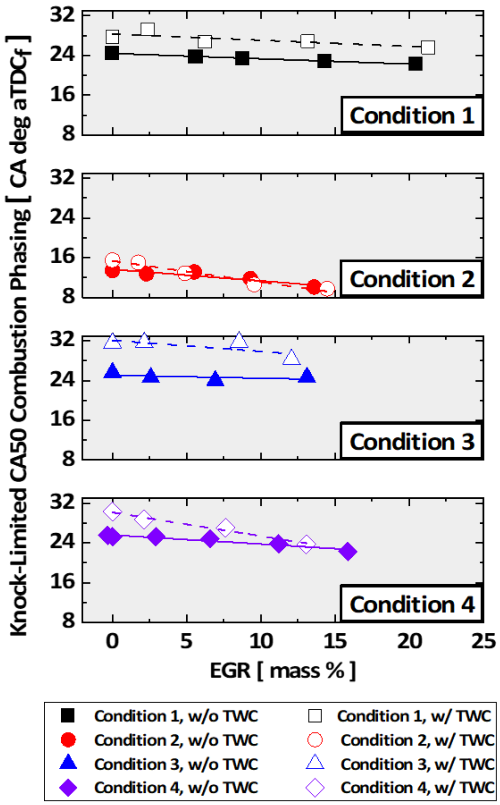

Figure 16. Knock-limited CA50 combustion phasing as a function of EGR at 1,500 rpm (Conditions 1-4) for both untreated EGR and TWC-treated EGR.

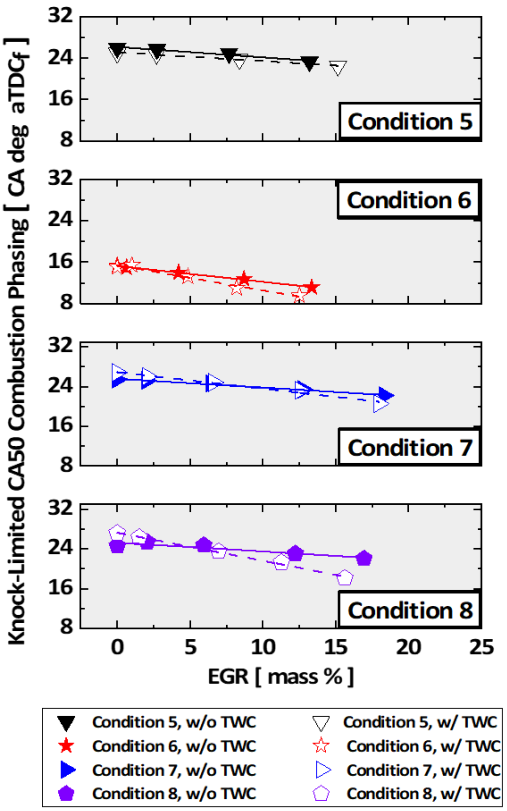

Figure 17. Knock-limited CA50 combustion phasing as a function of EGR at 3,000 rpm (Conditions 5-8) for both untreated EGR and TWC-treated EGR.

Table 5. Sensitivity of knock-limited combustion advance to EGR addition at each engine operating condition.

	No TWC / TWC	Advance of KL CA50 [CAD / % EGR]
Condition 1	No TWC	0.11
	TWC	0.13
Condition 2	No TWC	0.23
	TWC	0.43
Condition 3	No TWC	0.06
	TWC	0.22
Condition 4	No TWC	0.18
	TWC	0.48
Condition 5	No TWC	0.17
	TWC	0.20
Condition 6	No TWC	0.31
	TWC	0.49
Condition 7	No TWC	0.18
	TWC	0.33
Condition 8	No TWC	0.18
	TWC	0.57

These results are presented visually in bubble charts in Figure 18 and Figure 19, where the diameter of each bubble is proportional to the effectiveness of EGR on knock mitigation. For condition 1 (1,500 rpm, Figure 18) and Condition 5 (3,000 rpm, Figure 19), which are the highest load conditions each speed, the EGR shows only a modest effect at mitigating knock propensity. As the load is reduced in the other conditions, the effectiveness of the EGR at mitigating knock increases substantially. It is interesting that the knock mitigation effectiveness for the two lowest load conditions is similar, both at 1,500 rpm (Conditions 2 and 4, Figure 18), and at 3,000 rpm (Conditions 6 and 8, Figure 19) despite very different intake manifold temperatures and combustion phasing conditions. However, as shown in Figure 4, these conditions do experience very similar pressure-temperature trajectories, and therefore are subjected to very similar autoignition chemistry in the end gas, as was first pointed out by Szybist et al. [1].

Figure 18 and Figure 19 also provide an indication of the effect of untreated vs. TWC-treated EGR. The colored bubbles represent TWC-treated EGR and the black bubbles, which are overlaid on top of the colored bubbles, represent untreated EGR. In all cases, the TWC-treated EGR is more effective at mitigating knock. This finding agrees with the previous work from Lewis et al. [18], who decreased load as EGR was added to maintain a constant intake manifold density. Similar observations were also made from Fischer et al. [31] and from Pasternak et al. [32] who found that clean EGR provided a combustion phasing advance relative to untreated EGR. This provides an indication that the autoignition kinetics of the minor species in EGR are important for knock, and while this study does not provide evidence of which individual species are important for knock, there has been an extensive amount of prior work to indicate that NOx species [32-34] and acetylene [35] both promote autoignition.

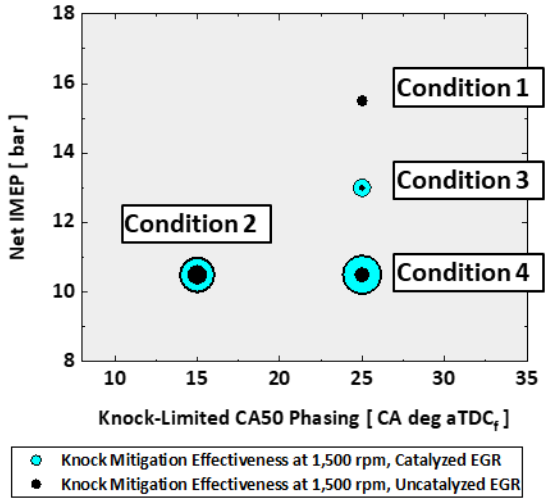

Figure 18. Bubble plots showing the effectiveness of EGR to mitigate knock at 1,500 rpm (Conditions 1-4) both with uncatalyzed and catalyzed EGR.

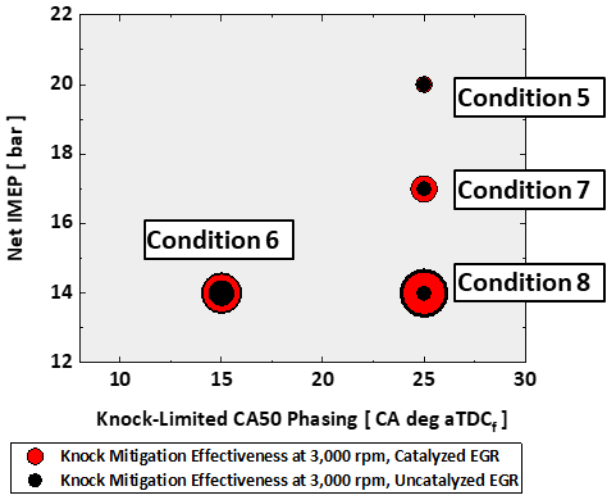

Figure 19. Bubble plots showing the effectiveness of EGR to mitigate knock at 3,000 rpm (Conditions 5-8) both with uncatalyzed and catalyzed EGR.

Discussion

Pressure-Temperature Regime

The results in this investigation confirm the earlier investigation by Szybist et al. [1] that EGR is less effective at mitigating knock under boosted conditions than it is under naturally-aspirated conditions. Further, this study demonstrates that the same trends exist across the engine speed range investigated, and these trends held with both types of EGR investigated. As a result, we can conclude that boosted engines are unable to realize the same benefits of EGR for knock mitigation to achieve higher efficiency in stoichiometric SI engines.

While the knock mitigation benefit is not as large under boosted operating conditions, there are still benefits of EGR that can be realized for higher efficiency, unrelated to knock. Specifically, as shown in Figure 11, the presence of EGR does increase γ, which provides an efficiency benefit. Further, the presence of EGR also decreases the exhaust temperature. At condition 5, the addition of EGR decreased the exhaust temperature by more than 66°C (from 822°C to 756°C), which agrees with prior studies [3-5]. The reduced exhaust temperature with EGR could be a more efficient way to reduce exhaust temperature for catalyst protection at high loads relative to protective enrichment, and it could also help to comply with increasingly stringent emission regulations because high levels of unburned emissions occur during enriched operation. Thus, while the knock mitigation benefits of EGR with boosted engines are not as large as with naturally aspirated engines, there may still be benefits that justify the use of technology in downsized boosted HPD production engines.

Untreated vs. TWC-Treated EGR

While the results from this investigation demonstrate that EGR treated with a TWC is more effective at mitigating knock than untreated EGR, there is not a complete understanding of why this is the case. As shown in Figure 10, treating the EGR with a catalyst decreases the concentrations of gaseous emissions which could be more reactive than the fresh charge of air and fuel.

To put this into perspective, Figure 20 and Figure 21 show the emission concentration of NO, acetylene, ethylene, and formaldehyde as a function of EGR at each operating condition as measured by FTIR. In all cases, the concentrations of these species are present in the exhaust and virtually eliminated by the TWC. For the hydrocarbon species (formaldehyde, ethylene, and acetylene), exhaust concentrations are between about 15-150 ppm, depending on operating condition and EGR level. Thus, at an EGR level of 20%, this translates to an increase in these species of 3-30 ppm, which is a very modest addition level for these species. For instance, in an investigation of homogeneous charge compression ignition (HCCI), Puranam and Steeper seeded acetylene into the intake charge at concentration that were two orders of magnitude higher (up to 2250 ppm) [35]. Zhao et al. sampled cylinder contents for HCCI combustion and reported a combustion phasing advance of less than 2 deg CA when ethylene and acetylene were increased by levels that were an order of magnitude higher than what is expected with 20% EGR (increases of approximately 200 ppm for ethylene and 100 ppm for acetylene). However, since these were HCCI studies, there is the possibility that the lower concentrations observed in this study could be more reactive under stoichiometric conditions.

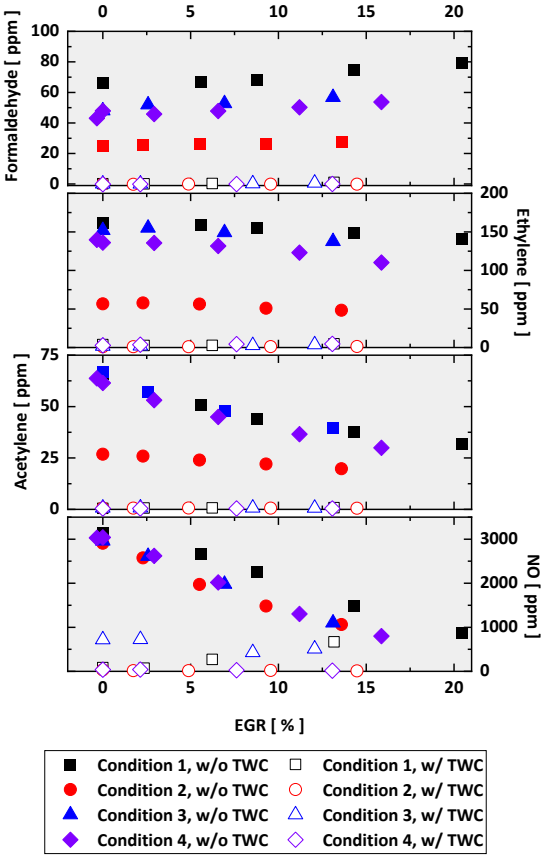

Figure 20. Emissions of NO, acetylene, ethylene, and formaldehyde with and without a TWC as a function of EGR at 1,500 rpm (Conditions 1-4).

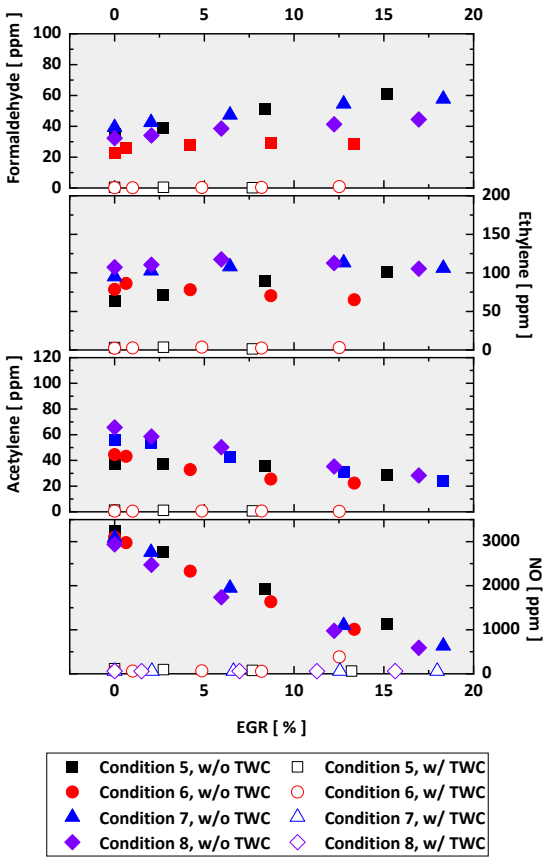

Figure 21. Emissions of NO, acetylene, ethylene, and formaldehyde with and without a TWC as a function of EGR at 3,000 rpm (Conditions 5-8).

Exhaust concentrations of NOx emissions are higher, but unlike the HC species, NOx concentrations are also a strong function of EGR. At an EGR rate of 20%, NO concentrations are roughly 750 ppm, which translates to approximately 150 ppm NO in-cylinder. The effect of NO concentration on knock phasing has been studied by Chen at al. [33] in an octane rating engine up to concentrations of 600 ppm. It was found that the impact of NO on knock phasing was dependent on fuel type. For alkanes, NO increased the knock propensity at low concentrations, but that the trend reversed at higher concentrations. In contrast, for aromatic fuels, there was a linear increase in knock propensity with NO across the range investigated. For all fuels, however, there was a net increase in knock propensity with NO concentrations of 150 ppm.

Based on these results, it is more likely that the increase in knock propensity is due to NO than unburned HC species. However, it is possible that there are combined effects and/or non-linear effects. Thus, research on this topic will continue by seeding individual components and measuring knock propensity. In addition, this work will be done in collaboration with the modeling efforts within the PACE consortium to be able to identify and model these effects so that the knock limited combustion phasing can be predictively modeled.

Conclusions

This investigation was conducted to expand on prior work that indicated that there was a kinetic limitation that prevented EGR from being as effective at mitigating knock under boosted conditions as it was under naturally aspirated conditions. As such, a wider range of operating conditions were investigated, including effect of engine speed (1,500 and 3,000 rpm), changing trajectory in the pressure-temperature domain by varying the intake manifold temperature (35, 60, and 90 deg C), and by considering the effect of minor species by studying the effect of untreated EGR vs. EGR that has been treated with a TWC. Additionally, the performance of a surrogate was also investigated to assess its appropriateness for future modeling studies. The following conclusions can be made:

- The knock-limited combustion phasing and cyclic variability of the surrogate fuel formulation reproduces that of the baseline gasoline across a wide range of operating conditions. Thus, this surrogate formulation is an appropriate representation of this gasoline for kinetic and CFD modeling purposes.
- This study confirmed the earlier findings that EGR is less effective at mitigating knock under boosted operating conditions relative to naturally aspirated conditions. This finding holds true at both engine speeds investigated, and with both untreated and TWC-treated EGR.
- EGR that has been treated with a TWC to remove the minor components is more effective at mitigating knock than EGR than hasn't been treated with a TWC. The effectiveness of the TWC-treated EGR is more than twice as effective at mitigating knock under some circumstances. This difference is most likely attributable to NOx components, but this will be confirmed in a future investigation.

References

1. Szybist, J.P., et al., *The Reduced Effectiveness of EGR to Mitigate Knock at High Loads in Boosted SI Engines.* Sae International Journal of Engines, 2017. **10**(5): p. 2305-2318.
2. Caton, J.A., *A Comparison of Lean Operation and Exhaust Gas Recirculation: Thermodynamic Reasons for the Increases of Efficiency*. SAE Technical Paper 2013-01-0266, 2013.
3. Duchaussoy, Y., A. Lefebvre, and R. Bonetto, *Dilution Interest on Turbocharged SI Engine Combustion*. SAE Technical Paper 2003-01-0629, 2003
4. Grandin, B. and H.-E. Ångström, *Replacing Fuel Enrichment in a Turbo Charged SI Engine: Lean Burn or Cooled EGR*. SAE Technical Paper 1999-01-3505, 1999.
5. Turner, J.W.G., et al., *Ultra Boost for Economy: Extending the Limits of Extreme Engine Downsizing*. SAE Int. J. Engines **7**(1):387-417, 2014.
6. Alger, T., et al., *The Interaction of Fuel Anti-Knock Index and Cooled EGR on Engine Performance and Efficiency.* SAE Int. J. Engines, 2012. **5**(3): p. 1229-1241.
7. Diana, S., et al., *Evaluation of the Effect of EGR on Engine Knock*. SAE Technical Paper 982479, 1998.
8. Grandin, B., et al., *Knock Suppression in a Turbocharged SI Engine by Using Cooled EGR*. SAE Technical Paper 982476, 1998.

9. Hwang, K., et al., *Development of New High-Efficiency Kappa 1.6L GDI Engine*. SAE Technical Paper 2016-01-0667, 2016.
10. Hakariya, M., T. Toda, and M. Sakai, *The New Toyota Inline 4-Cylinder 2.5L Gasoline Engine*. SAE Technical Paper 2017-01-1021, 2017.
11. Matsuo, S., et al., *The New Toyota Inline 4 Cylinder 1.8L ESTEC 2ZR-FXE Gasoline Engine for Hybrid Car*. SAE Technical Paper 2016-01-0684, 2016.
12. Kargul, J., et al., *Benchmarking a 2018 Toyota Camry 2.5-Liter Atkinson Cycle Engine with Cooled-EGR*. SAE Technical Paper 2019-01-0249, 2019.
13. Lee, B., et al., *Development of High Efficiency Gasoline Engine with Thermal Efficiency over 42%.* SAE Technical Paper 2017-01-2229, 2017.
14. Szybist, J., et al., *What Fuel Properties Enable Higher Thermal Efficiency in Spark-Ignited Engines?* Progress in Energy and Combustion Science, 2020. Accepted for Publication.
15. Agency, U.S.E.P., *The 2018 EPA Automotovie Trends Report: Greenhouse Gas Emissions, Fuel Economy, and Technology since 1975*. 2019, United States Environmental Protection Agency.
16. Colias, M., *GM, Volkswagen Say Goodbye to Hybrid Vehicles*, in *The Wall Street Journal*. 2019.
17. Hoepke, B., et al., *EGR Effects on Boosted SI Engine Operation and Knock Integral Correlation*. SAE Technical Paper 2012-01-0707, 2012.
18. Lewis, A., et al., *Observations on the Measurement and Performance Impact of Catalyzed vs. Non Catalyzed EGR on a Heavily Downsized DISI Engine*. SAE Technical Paper 2014-01-1196, 2014.
19. Splitter, D.A. and J.P. Szybist, *Experimental Investigation of Spark-Ignited Combustion with High-Octane Biofuels and EGR. 2. Fuel and EGR Effects on Knock-Limited Load and Speed.* Energy & Fuels, 2014. **28**(2): p. 1432-1445.
20. ASTM D2699-18a, Standard Test Method for Research Octane Number of Spark-Ignition Engine Fuel. ASTM International, West Conshohocken, PA, 2018.
21. Kalghatgi, G.T., *Fuel Anti-Knock Quality - Part I. Engine Studies*. SAE Technical Paper 2001-01-3584, 2001.
22. Szybist, J.P. and D.A. Splitter, *Pressure and temperature effects on fuels with varying octane sensitivity at high load in SI engines.* Combustion and Flame, 2017. **177**: p. 49-66.
23. Szybist, J.P. and D.A. Splitter, *Understanding chemistry-specific fuel differences at a constant RON in a boosted SI engine.* Fuel, 2018. **217**: p. 370-381.
24. Prikhodko, V.Y., et al., *Ammonia Generation over TWC for Passive SCR NOX Control for Lean Gasoline Engines*. 2014, SAE Technical Paper 2014-01-1505.
25. Yun, H.J. and W. Mirsky, *Schlieren-Streak Measurements of Instantaneous Exhaust Gas Velocities from a Spark-Ignition Engine*. SAE Technical Paper 741015, 1974.
26. Chun, K.M. and J.B. Heywood, *Estimating Heat-Release and Mass-of-Mixture Burned from Spark-Ignition Engine Pressure Data.* Combustion Science and Technology, 1987. **54**(1-6): p. 133-143.
27. Wagnon, S.W., et al., *Experimental and Modeling Study of the Ignition of a Standard Oxygenated Gasoline Fuel.* TBD - Paper in preparation, 2020.
28. Alger, T., et al., *The Impact of Cooled EGR on Peak Cylinder Pressure in a Turbocharged, Spark Ignited Engine*. SAE Technical Paper 2015-01-0744, 2015.
29. Chang, Y. and J.P. Szybist. *Fuel Effects on Combustion with EGR Dilution in Spark Ignited Engines*. in *The 2016 Spring Technical Meeting of the Central States Section of the Combustion Institute (CSSCI 2016)*. 2016. Knoxville, TN: CCSI 145IC-0082.
30. Szybist, J.P. and D. Splitter, *Effects of Fuel Composition on EGR Dilution Tolerance in Spark Ignited Engines.* SAE Int. J. Engines, 2016. **9**(2): p. 819-831.
31. Fischer, M., et al., *Clean EGR for Gasoline Engines – Innovative Approach to Efficiency Improvement and Emissions Reduction Simultaneously*. SAE Technical Paper 2017-01-0683.
32. Pasternak, M., et al. *Simulation of the Effects of Spark Timing and External EGR on Gasoline Combustion Under Knock-Limited Operation at High Speed and Load*. 2018. Cham: Springer International Publishing.
33. Chen, Z.Y., et al., *The impact of nitric oxide on knock in the octane rating engine.* Fuel, 2019. **235**: p. 495-503.
34. Chen, Z.Y., et al., *Impact of nitric oxide (NO) on n-heptane autoignition in a rapid compression machine.* Combustion and Flame, 2017. **186**: p. 94-104.
35. Puranam, S.V. and R.R. Steeper, *The Effect of Acetylene on Iso-octane Combustion in an HCCI Engine with NVO*. SAE Technical Paper 2012-01-1574, 2012.

Contact Information

szybistjp@ornl.gov

Acknowledgments

This research was conducted as part of the Partnership to Advance Combustion Engines (PACE) Consortium sponsored by the U.S. Department of Energy (DOE) Vehicle Technologies Office (VTO). The PACE Consortium is a collaborative project of multiple National Laboratories that combines unique experiments with world-class DOE computing and machine learning expertise to speed discovery of knowledge, improve engine design tools, and enable market-competitive powertrain solutions with potential for best-in-class lifecycle emissions. A special thanks to DOE VTO program managers Mike Weismiller and Gurpreet Singh.

A special thanks also to Brian Kaul at ORNL for his development of the engine controller, data acquisition system, and the Oak Ridge Combsution Analysis System (ORCAS), and to Flavio Dal Forno Chuahy for his help in blending the surrogate fuel, engine system troubleshooting, and generating Figure 1.

Definitions/Abbreviations

aTDC$_f$	After top dead center firing
BMEP	Brake mean effective pressure
CA	Crank angle
CA50	Crank angle at which 50% of fuel heat release
CAD	Crank angle degree
CFD	Computation fluid dynamics
COV	Coefficient of variation
EGR	Exhaust gas recirculation
HCCI	Homogeneous charge compression ignition
HPD	High power density
IMEP	Indicated mean effective pressure
LPD	Low power density

MAPO	Maximum amplitude of pressure oscillation
ORCAS	Oak Ridge Combustion Analysis System
PACE	Partnership for Advancing Combustion Engines
RON	Research octane number
TWC	Three-way catalyst
γ	Ratio of specific heats